

OMTN, Volume 11

## **Supplemental Information**

### **miR-1266 Contributes to Pancreatic Cancer Progression and Chemoresistance by the STAT3 and NF- $\kappa$ B Signaling Pathways**

**Xin Zhang, Dong Ren, Xianqiu Wu, Xi Lin, Liping Ye, Chuyong Lin, Shu Wu, Jinrong  
Zhu, Xinsheng Peng, and Libing Song**

## Supporting Information

### **Figure S1. miR-1266 is upregulated in pancreatic cancer and correlated with poor prognosis.**

(a) miR-1266 expression levels was markedly elevated in pancreatic cancer tissues compared with normal pancreatic tissues as assessed by analyzing the TCGA pancreatic cancer miRNA sequencing dataset (Normal, n = 4; Pancreatic cancer, n = 178).  $P < 0.001$ . (b) miR-1266 expression levels was elevated in pancreatic cancer tissues compared with normal pancreatic tissues as assessed by analyzing the pancreatic cancer miRNA expression profiling from E-GEOD-32678 dataset (Normal, n = 7; Pancreatic cancer, n = 25).  $P < 0.05$ . (c and d) Kaplan–Meier analysis of overall and progression-free survival curves of patients with pancreatic cancer with high miR-1266 expression versus low miR-1266 expression in the TCGA pancreatic cancer dataset. The best cutoff point was chosen by using X-tile software with log-rank test.

### **Figure S2. The correlation of chemotherapeutic response with overall and progression-free survival in pancreatic cancer patients.**

(a and b) Kaplan–Meier analysis of overall (a) and progression-free (b) survival curves of patients with pancreatic cancer with PD/SD versus CR/PR.  $P < 0.001$ , (c and d) Kaplan–Meier analysis of overall (c) and progression-free (d) survival curves of patients with pancreatic cancer with PD/SD versus CR/PR in the TCGA dataset.  $P < 0.001$ .

### **Figure S3. miR-1266 promotes chemoresistance in pancreatic cancer cells in vitro.**

(a) Real-time PCR analysis of miR-1266 expression in pancreatic cancer cells transduced with miR-1266 or transfected with anta-1266 compared to controls. Transcript levels were normalized by *U6* expression. Error bars represent the mean  $\pm$  s.d. of three independent experiments.  $*P < 0.05$ . (b) Inhibition of miR-1266 increased the apoptotic ratio in the absence of GEM. Error bars represent the mean  $\pm$  s.d. of three independent experiments.  $*P$

< 0.05. **(c)** Annexin V-FITC/PI staining of the indicated cells treated with gemcitabine (10  $\mu$ M) for 36 h. Error bars represent the mean  $\pm$ S.D. of three independent experiments. \**P* < 0.05. **(d)** The JC-1 staining showed that silencing miR-1266 decreased the mitochondrial potential in a dose-dependent manner in pancreatic cancer cells. Error bars represent the mean  $\pm$ S.D. of three independent experiments. \**P* < 0.05. **(e and f)** Analysis of the activities of caspase-9 **(e)** and caspase-3 **(f)** were detected by the cleaved forms of these two proteins. Error bars represent the mean  $\pm$ S.D. of three independent experiments. \**P* < 0.05. **(g)** Western blotting analysis of Bcl-2, Bcl-xL, Mcl-1 and Survivin in the indicated cells. **(h)** The effect of miR-1266 on proliferation of pancreatic cancer cells was assessed by MTT assay.

**Figure S4. Inhibition of miR-1266 sensitizes pancreatic cancer cells to gemcitabine in**

**vivo.** **(a)** Xenograft model in nude mice. Representative images of tumor-bearing mice on day 10 and day 45 in AsPC-1 cells. Mice were euthanized, and tumors from each experimental group were excised. **(b)** After 10 days of inoculating AsPC-1 cells, mice were intraperitoneal injected with 50  $\mu$ g/g gemcitabine (GEM) two times each week for 4 weeks. Tumor volumes in the low-dose anta-1266, high-dose anta-1266 and scramble groups were measured from the fifth day at five days interval. Data presented are the mean  $\pm$  s.d. **(c)** Tumor weights of each group. **(d)** The overall survival of mice in the indicated group. **(e)** After 10 days of inoculating PANC-1 cells, mice were intraperitoneal injected with 50  $\mu$ g/g gemcitabine (GEM) two times each week for 4 weeks. Tumor volumes in the high-dose anta-1266 and control groups were measured from the fifth day at five days interval. Data presented are the mean  $\pm$  s.d. **(f)** Tumor weights of each group. **(g)** The Caspase-3 activity in the tumor tissues formed by the low-dose anta-1266, high-dose anta-1266 and scramble groups in AsPC-1 and PANC-1 cells respectively. **(h)** After 10 days of inoculating BxPC-3 cells, mice were intraperitoneal injected with 50  $\mu$ g/g gemcitabine (GEM) two times each week for 4 weeks. Tumor volumes in the miR-1266-overexpressing and control groups were

measured from the fifth day at five days interval. Data presented are the mean  $\pm$  s.d. **(i)** Tumor weights of each group. **(j)** Western blotting of SOCS3, PTPN11, ITCH and TNIP1 expression in scramble and anta-1266 (H.D.) tumor groups.  $\alpha$ -Tubulin served as the loading control.

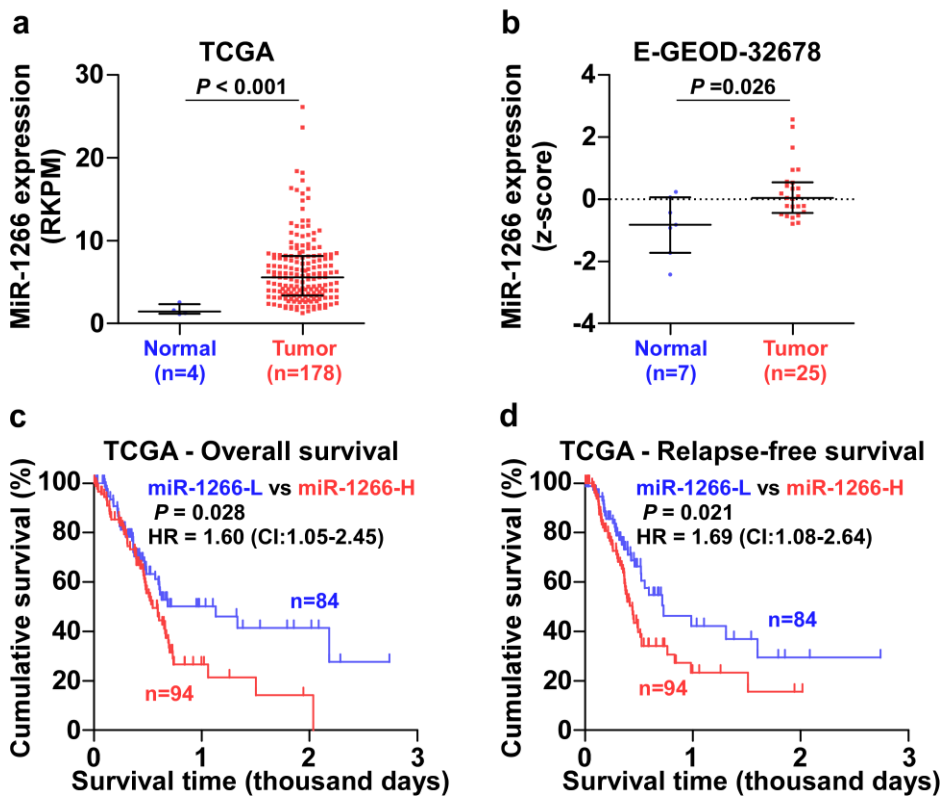
**Figure S5. The inhibitors of STAT3 signaling Stattic and S3I-201 and the inhibitors of NF- $\kappa$ B signaling LY2409881 and JSH-23 repress STAT3 and NF- $\kappa$ B activity in a dose-dependent manner in pancreatic cancer cells.** **(a-d)** STAT3 inhibitors Stattic and S3I-201, or NF- $\kappa$ B inhibitors LY2409881 and JSH-23 showed potent inhibition of the STAT3 and NF- $\kappa$ B reporter activities in pancreatic cancer cells. Error bars represent the mean  $\pm$  s.d. of three independent experiments. \* $P < 0.05$ .

**Figure S6. Wild-type sequence and mutant sequences of 3'UTRs in SOCS3, PTPN11, ITCH and TNIP1.** **(a)** Predicted miR-1266 targeting sequence and mutant sequences in 3' UTRs of SOCS3, PTPN11, ITCH and TNIP1. **(b and c)** Individual silencing of these targets rescued the STAT3 (E) and NF- $\kappa$ B (F) activity repression in miR-1266-silencing cells.

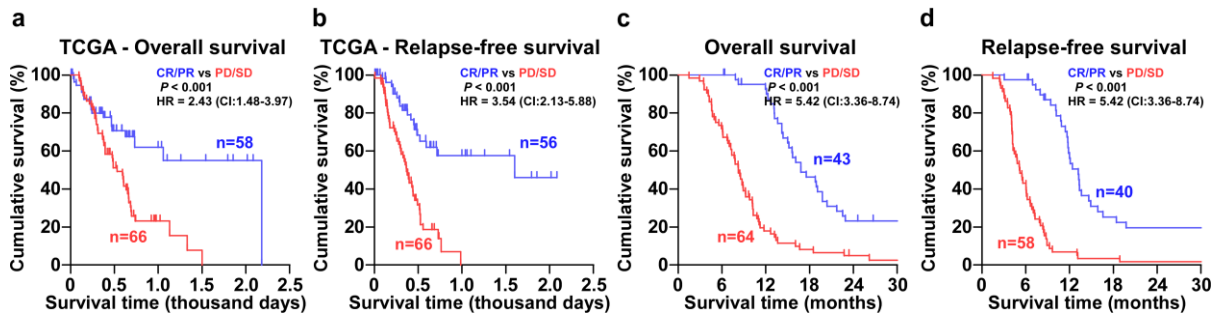
**Figure S7. Recurrent gains and hypomethylation contribute to miR-1266 overexpression in pancreatic cancer tissues.** **(a)** The percentage of deletion, diploid and gain in the pancreatic cancer samples from TCGA. **(b)** The average expression level of miR-1266 in pancreatic cancer patients with gains was higher than those without gains in the pancreatic cancer dataset TCGA. Each bar represents the median values  $\pm$  quartile values. **(c)** The percentage of deletion, diploid and gain in our pancreatic cancer samples, ANT and benign pancreatic lesions. **(d)** The average expression level of miR-1266 in pancreatic cancer tissues with gains was higher than those without gains. Each bar represents the median values  $\pm$  quartile values. **(e)** Methylation level of miR-1266 promoter in the pancreatic cancer

dataset from TCGA. (f) Methylation level of miR-1266 promoter using cg06706204 in our pancreatic cancer tissues, ANT and benign pancreatic lesions. Methylation ratio: methylation percentage in each tissue. (g) Real-time PCR analysis of miR-1266 expression levels in pancreatic cancer tissues with different methylation ratio. Transcript levels were normalized to *U6* expression.

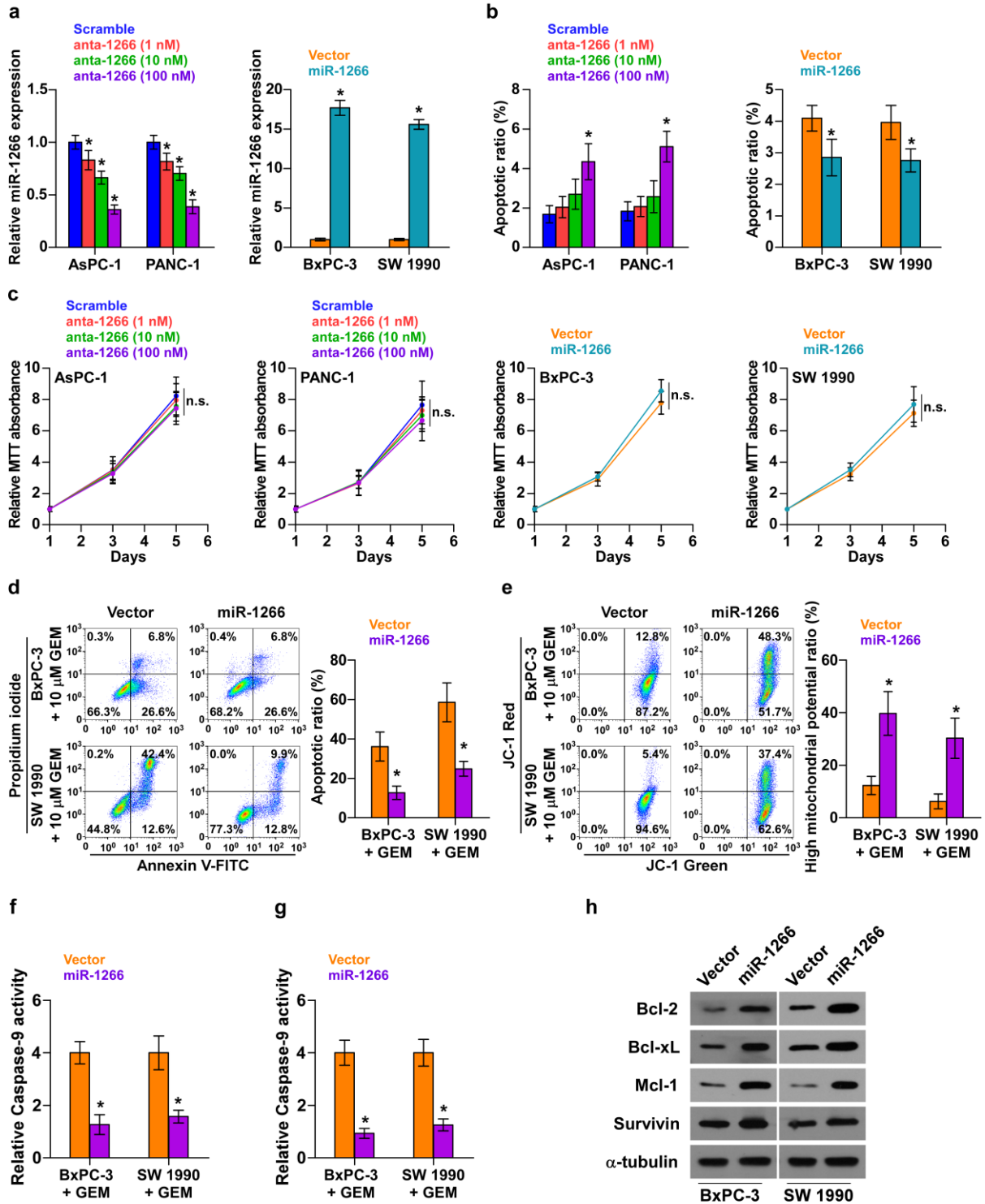
### Supplement figure 1



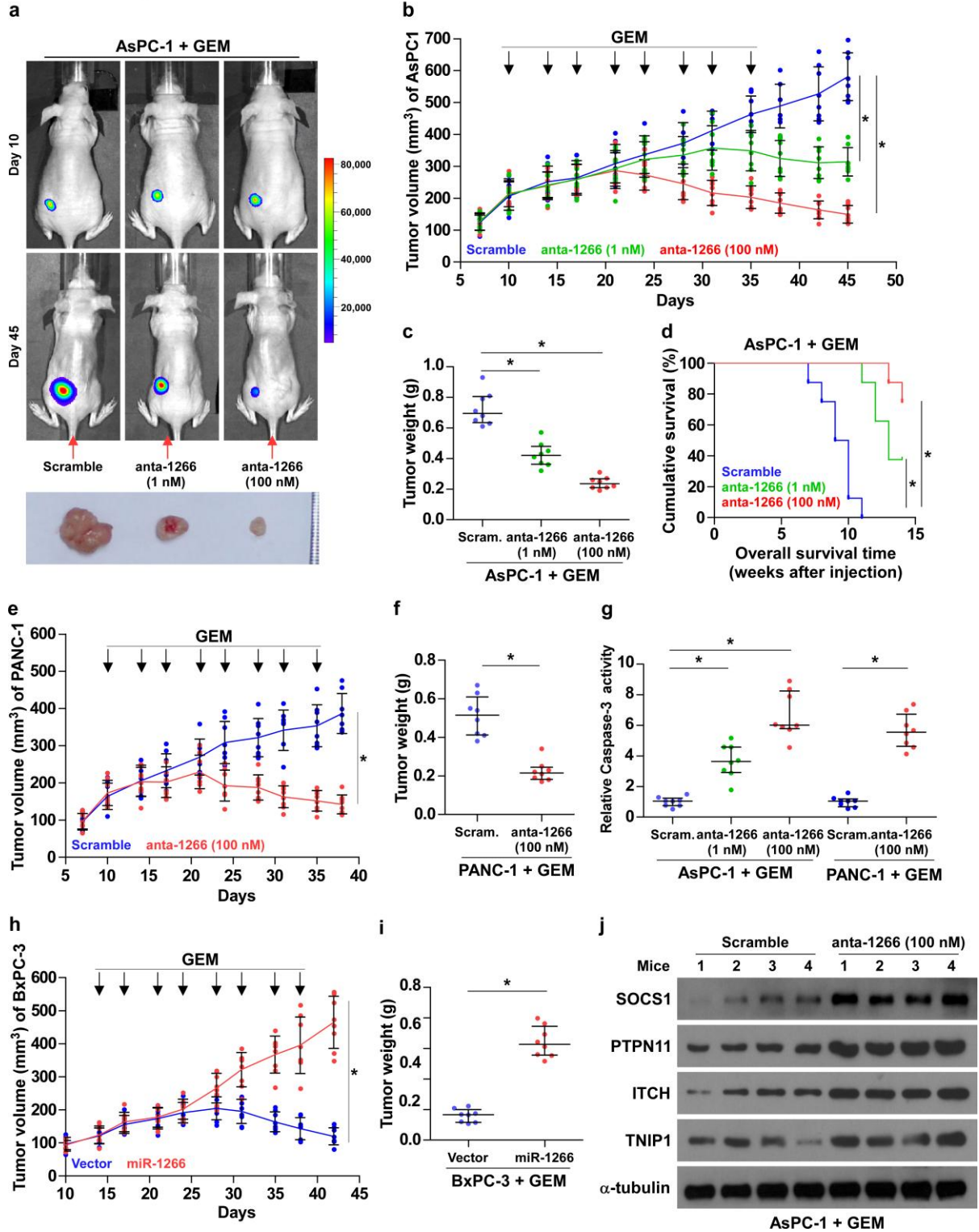
### Supplement figure 2



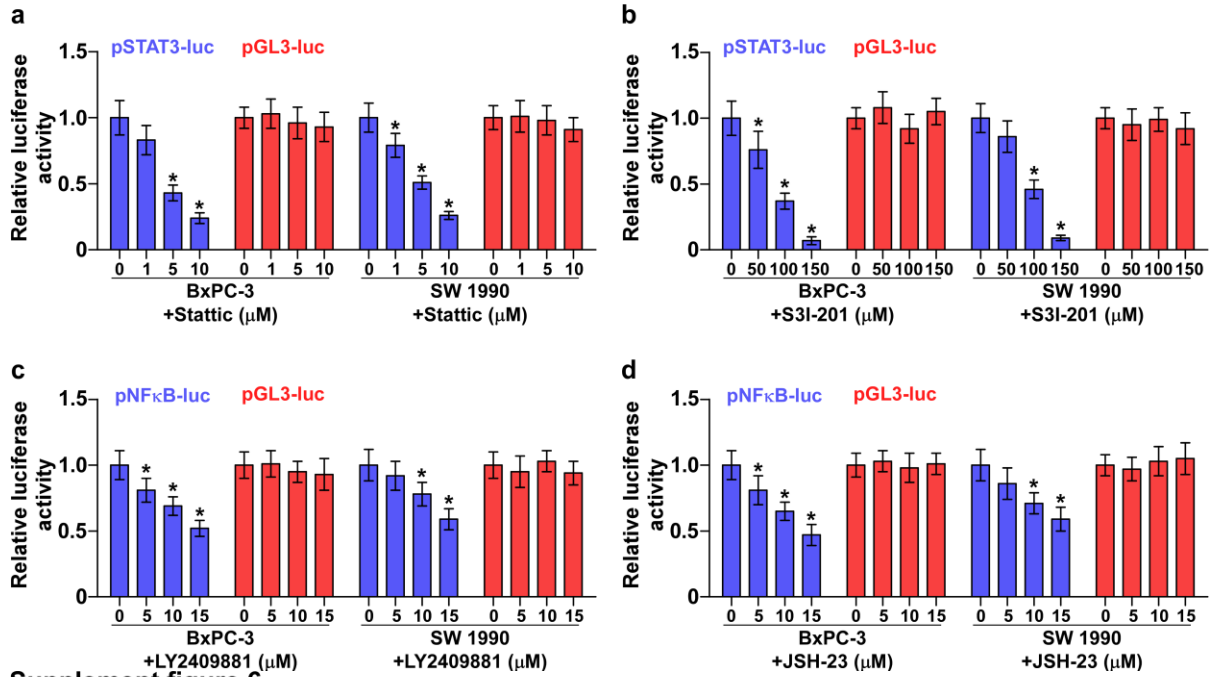
### Supplement figure 3



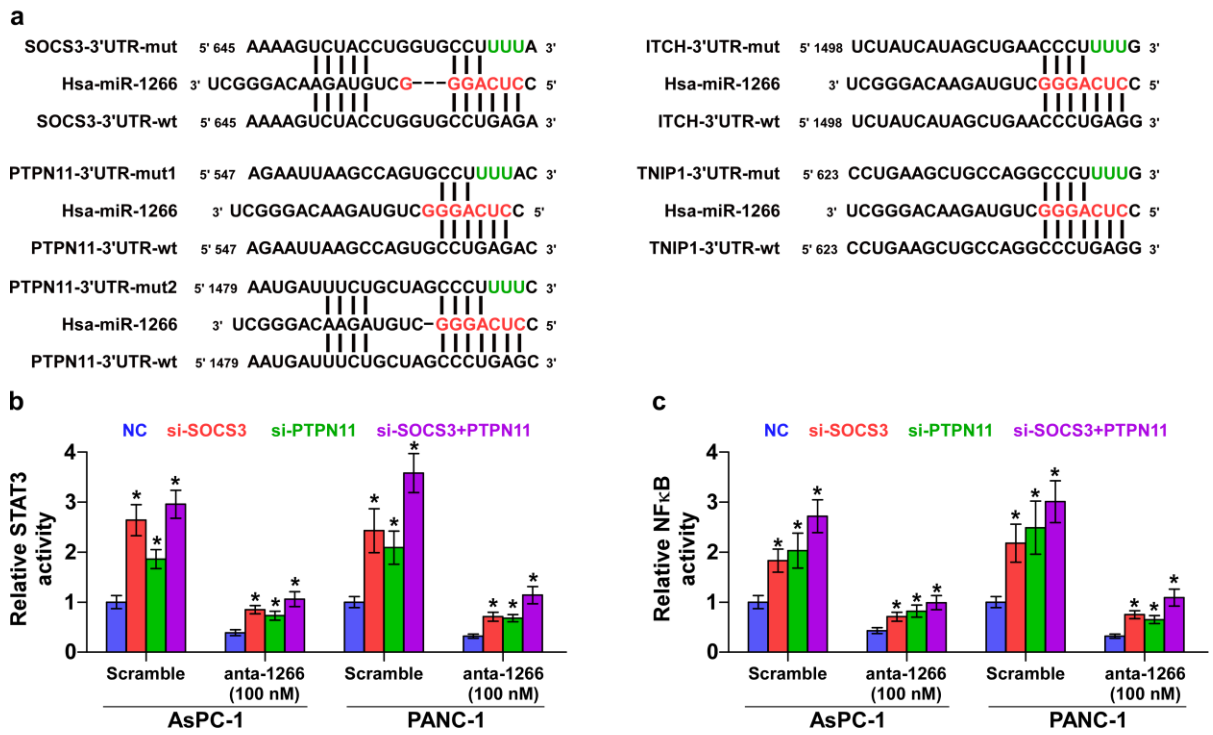
Supplement figure 4



**Supplement figure 5**



**Supplement figure 6**





Supplement figure 7

